

Electronic Supplementary Information

Regulation of the cathode for amphi-charge storage in a redox electrolyte for high-energy lithium-ion capacitors

Yunlong Zhang,^a Huixia Chao,^a Haiyan Liu,^b Xiaoshan Wang,^a Wei Xing,^a Han Hu^{*a}
and Mingbo Wu^{*a}

a. State Key Laboratory of Heavy Oil Processing, Institute of New Energy, College of
Chemical Engineering, China University of Petroleum (East China), Qingdao 266580,
China.

b. YanKuang Group Co., Ltd. New Energy Division, Zoucheng, 273500, China.

Corresponding authors: hhu@upc.edu.cn; wumb@upc.edu.cn

Experimental Section

Materials and reagents

Activated charcoal (C112241, CAS:7440-44-0), Lithium carbonate (purity \geq 99.0%, L101681, CAS: 554-13-2), Titanium oxide (purity \geq 99.0%, T164497, CAS: 13463-67-7), Lithium iodide (purity \geq 99%, L106780, CAS: 10377-51-2) and Lithium nitrate (purity \geq 99.9%, L100138, CAS: 7790-69-4) were purchased from Aladdin Industrial Corporation. LiTFSI (Lithium bis(trifluoromethanesulfonyl)imide) (Product number: 9100301) and DEGDME (Diethylene glycol dimethyl ether) (Product number: 9201801) were purchased from DoDoChem. All the chemicals were used as received without further purification. The deionized water was produced by a Millipore system in our lab.

Synthesis of nanostructured lithium titanate

The lithium titanate (LTO) particles were prepared according to previous research.

[1] The $\text{Li}_4\text{Ti}_5\text{O}_{12}$ was prepared by calcining the mixture of TiO_2 particles and Li_2CO_3 (the Li/Ti mole ratio was 0.4) at 900 °C for 20 h in air.

Materials characterization

The morphology was observed using scanning electron microscopy (SEM, Hitachi S4800) and transmission electron microscopy (TEM, JEM-2100UHR). The crystal structure was determined using X-ray diffraction (X' Pert PRO MPD). The nitrogen sorption isotherms were recorded on a physisorption analyzer (Micromeritics TriStar II 3020). The specific surface area was obtained via the Brunauer-Emmett-Teller (BET) analysis. The pore size distribution was determined using the Barrett-Joyner- Halenda (BJH) model.

Electrochemical measurement

To evaluate the electrochemical performance, the working electrode was firstly fabricated using the following procedure. The cathode was constructed by casting AC (80 wt.%), carbon black (10 wt.%), and polyvinyl difluoride (10 wt.%) dispersed in the N-methyl-2-pyrrolidone (NMP) on the Al foil, followed by vacuum drying at 80 °C for 12 h. As for the fabrication of the anode, the AC was replaced with LTO and the Cu foil, instead of the Al foil, was employed as the current collector. The electrochemical performance of the electrodes was evaluated using the coin cells with lithium foil as the counter and reference electrodes, 1 M LiTFSI in DEGDME as the electrolyte and a glass fiber film as the separator. To explore the electrolyte-enabled capacity, LiI was introduced into the catholyte with a concentration of 50 mM. To evaluate the electrochemical performance of the lithium-ion capacitors (LICs), three-electrode split cell was used where the lithium wire was used as the reference electrode in addition to the cathode and anode. To modulate the E_{OV} , the reference electrode and the cathode or anode were firstly discharged/charged for a few cycles and then regulated to the preset potential, for example 2 V vs Li/Li⁺, similar to the method reported in ref. 2. After holding at this potential for a while, the potential of both electrodes would be stabilized. Then, the cathode and anode were connected for electrochemical performance evaluation. As for the LICs with redox electrolyte, the asymmetric electrolyte design has been designed. Specific, the LiTFSI in DEGDME electrode was used for the anode while the normal electrolyte with extra LiI was employed for the cathode. The cyclic voltammetry (CV) profiles and the galvanostatic charge and discharge (GCD) tests

were recorded using an IVIUM multi-channel electrochemical workstation. The rate capability and cyclic performance were tested using a Land battery tester.

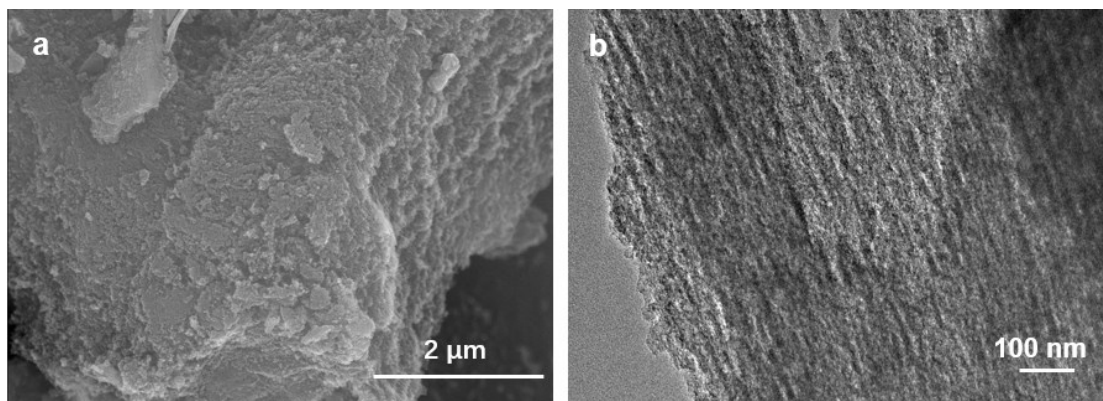


Figure S1 (a) SEM image and (b) TEM image of the AC.

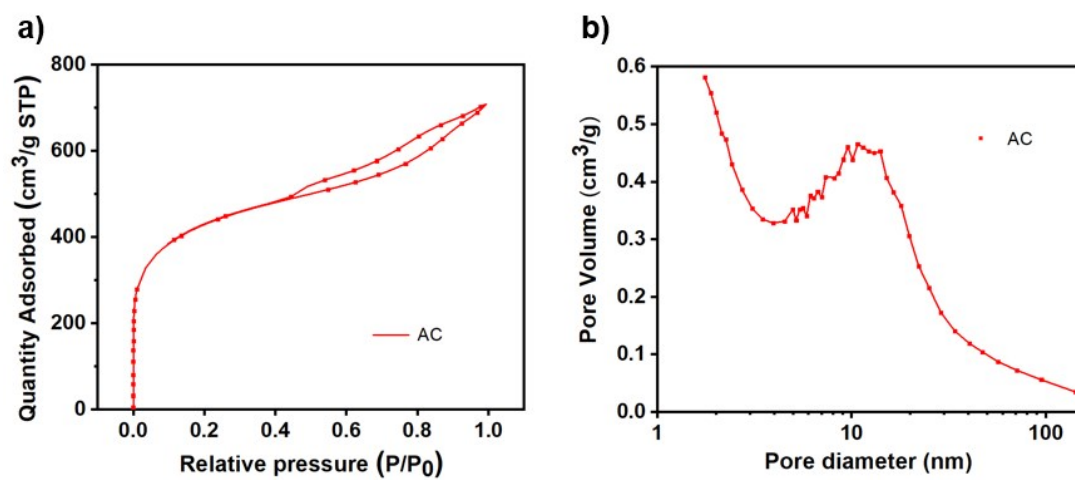


Figure S2 (a) N₂ sorption isotherm and (b) pore-size distribution of the AC.

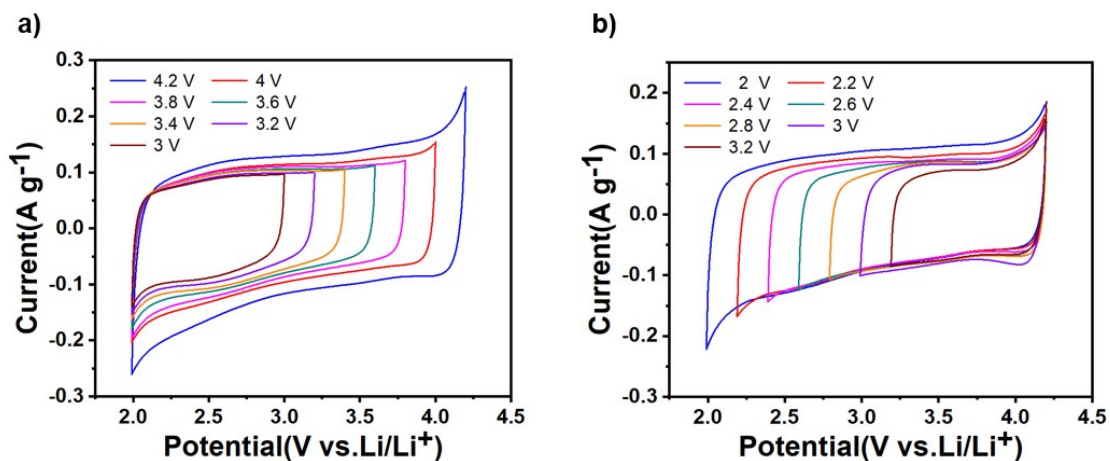


Figure S3 Electrochemical evaluation of the AC cathode in an electrolyte of 1 M LiTFSI in DEGDME in various potential windows between 2.0 and 4.2 V vs Li/Li⁺. CV curves at different potential range (a) from 2.0 to 4.2 V and (b) from 4.2 to 2.0 V with an interval of 0.2 V at a scan rate of 2 mV s⁻¹. The color code is related to the cutoff potential during the CV tests.

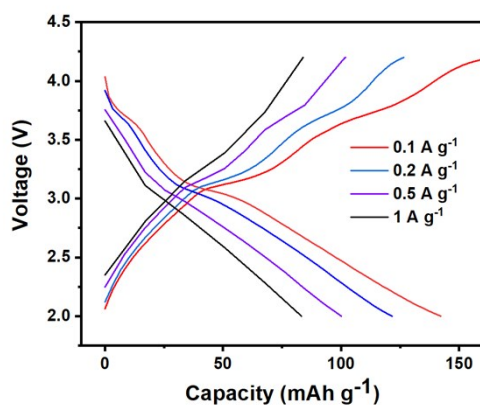


Figure S4 GCD profiles of AC/Li half-cell in an electrolyte containing 50 mM LiI as the redox additive.

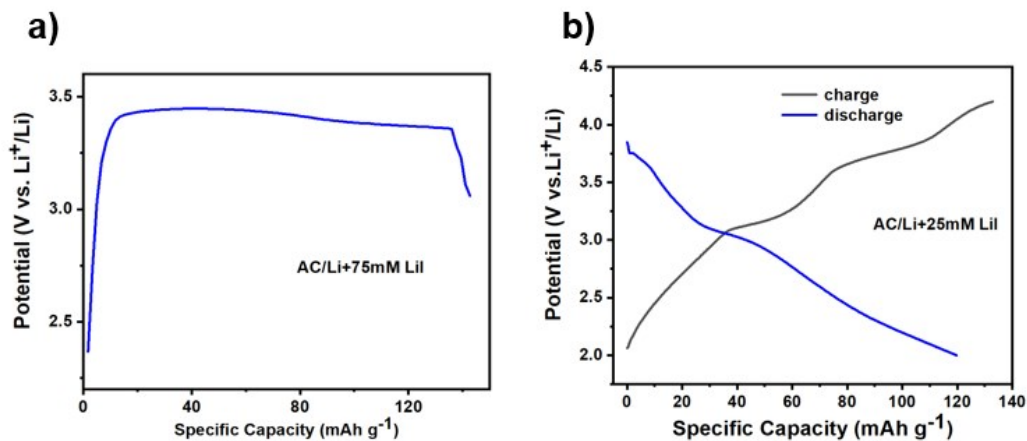


Figure S5 GCD profiles of the AC/Li half-cell with the electrolyte containing (a) 75 mM and (b) 25 mM LiI as the redox additive at a current density of 0.1 A g^{-1} .

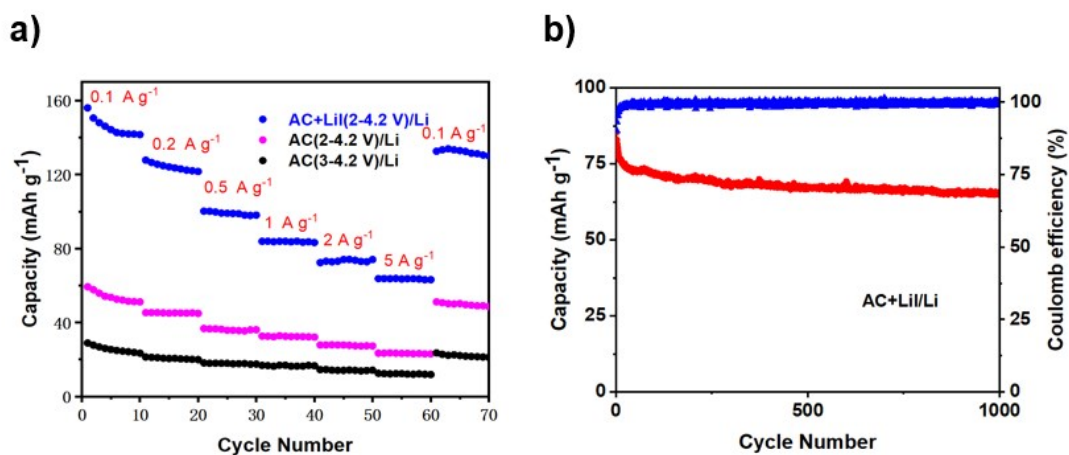


Figure S6 (a) Comparison of the specific capacity of the AC cathodes in a half cell with different operation conditions. (b) Cyclic performance of the AC cathode operated in the electrolyte with the redox additive at a current density of 2 A g^{-1} .

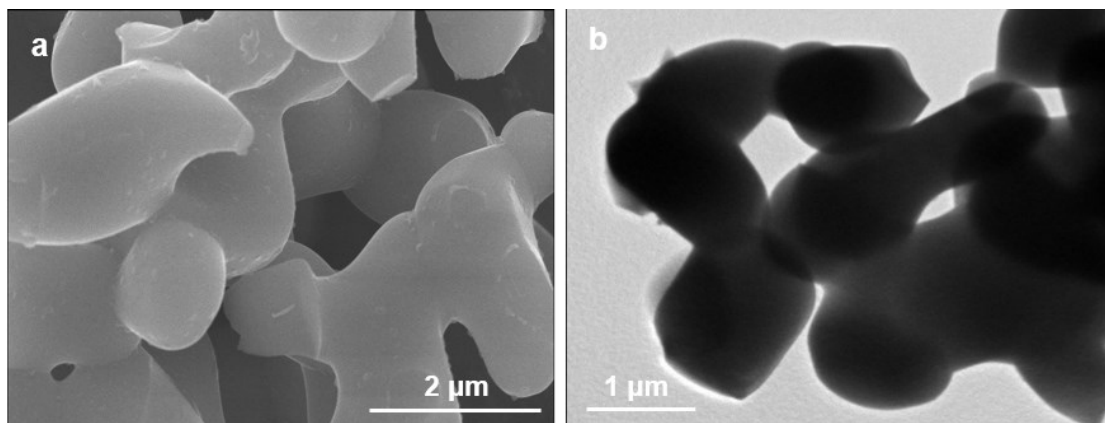


Figure S7 (a) SEM image and (b) TEM image of as-prepared $\text{Li}_4\text{Ti}_5\text{O}_{12}$.

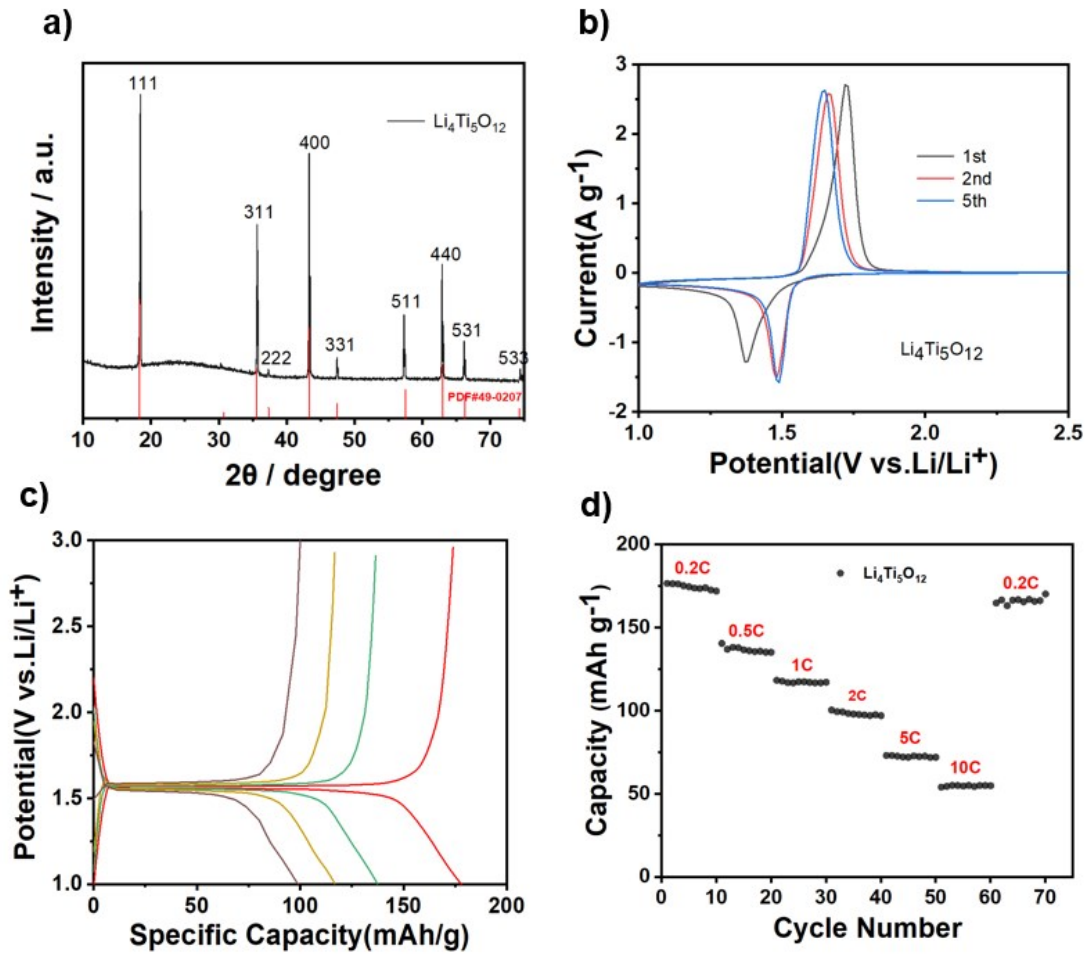


Figure S8 (a) XRD pattern of the $\text{Li}_4\text{Ti}_5\text{O}_{12}$. (b) CV curves of the LTO electrode of different cycles at a scan rate of 1 mV s^{-1} . (c) GCD profiles of the LTO electrode at a current density of 0.1 A g^{-1} . (d) Rate capability of the LTO electrode under different current rates: 0.2, 0.5, 1, 2, 5, and 10 C (1 C = 160 mAh g^{-1});

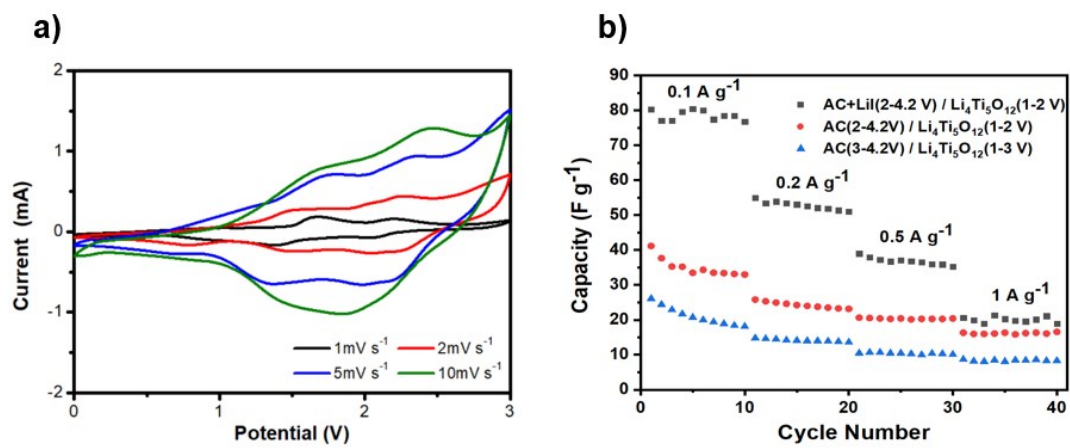


Figure S9 (a) CV curves of the AC/L₄Ti₅O₁₂ LTO with the LiI additive in the catholyte.

(b) Comparison of electrochemical performance of the three different LICs.

Table S1 Comparison of electrochemical performance of typical LICs with an AC cathode and the LTO-based anode.

Cathode material	Anode material	Electrolyte	Capacitance	Energy Density (Wh kg ⁻¹)	Ref.
AC	Graphene sheets wrapped nano-Li ₄ Ti ₅ O ₁₂	1 M LiPF ₆ in EC: DMC (1:1)	80 F g ⁻¹	30	[3]
AC	Li ₄ Ti ₅ O ₁₂ /T ₂	1 M LiPF ₆ in EC: DMC (1:1)	N.M.	65	[4]
AC	Li ₄ Ti ₅ O ₁₂ -graphene	1 M LiPF ₆ in EC: DMC: DEC (1:1:1)	15 F g ⁻¹	50	[5]
AC	Spinel Li ₄ Ti ₅ O ₁₂ spheres	1 M LiPF ₆ in EC: DMC (1:1)	80 F g ⁻¹	74.3	[6]
AC	Carbon-modified Li ₄ Ti ₅ O ₁₂ -C nano-composite	1 M LiPF ₆ in EC: DMC (1:3)	22 F g ⁻¹	20	[7]
Graphene-sucrose	Graphene-inserted Li ₄ Ti ₅ O ₁₂	1 M LiPF ₆ in EC: DMC (1:1)	N.M.	95	[8]
AC	Li ₄ Ti ₅ O ₁₂	1 M LiTFSI in DEGDME with 50 mM LiI	80 F g ⁻¹	99.8	This work

Reference

- 1 H. Jung, S. Myung, C. Yoon, S. Son, K. Oh, K. Amine, B. Scrosati, Y. Sun, *Energy Environ. Sci.*, 2011, **4**, 1345-1351.
- 2 Z. Weng, F. Li, D. Wang, L. Wen, H. Cheng, *Angew. Chem. Int. Ed.*, 2013, **52**, 3722-3725.
- 3 T. Yuan, W. Li, W. Zhang, Y. He, C. Zhang, X. Liao, Z. Ma, *Ind. Eng. Chem. Res.*, 2014, **53**, 10849-10857.
- 4 S. Dsoke, B. Fuchs, E. Gucciardi, M. W. Mehrens, *J. Power Sources*, 2015, **282**, 385-393.
- 5 N. Xu, X. Sun, X. Zhang, K. Wang, Y. Ma, *RSC Adv.*, 2015, **5**, 94361-94368.
- 6 S. Deng, J. Li, S. Sun, H. Wang, J. Liu, H. Yan, *Electrochim. Acta*, 2014, **146**, 37-43.
- 7 J. Ni, L. Yang, H. Wang, L. Gao, *J. Solid State Electrochem.*, 2012, **16**, 2791-2796.
- 8 K. Leng, F. Zhang, L. Zhang, T. Zhang, Y. Wu, Y. Lu, Y. Huang, Y. Chen, *Nano Res.*, 2013, **6**, 581-592.